

Revisiting the real graviton effects at CERN LHC within the quantum gravity theory with large extra dimensions

Xing-Gang Wu* and Zhen-Yun Fang

Department of Physics, Chongqing University, Chongqing 400044, People's Republic of China

(Received 6 October 2008; published 3 November 2008)

CERN LHC provides a good experimental platform to perturbatively probe the fundamental gravity scale up to several TeV, with the precise value depending on the number of extra dimensions. The leading experimental signal of the graviton at the LHC is from the process $pp \rightarrow \text{jet} + \cancel{E}_T$, where \cancel{E}_T stands for the transverse missing energy. A detailed discussion on the hadronic production of the real graviton through hard subprocesses: $q\bar{q} \rightarrow G + g$, $g + q \rightarrow G + q$, and $g + g \rightarrow G + g$ have been studied within the quantum gravity theory with large extra dimensions. The main theoretical uncertainties together with the dominant standard model background to these processes, e.g. $q\bar{q} \rightarrow Z^0 + g$ and $g + q \rightarrow Z^0 + q$ with Z^0 further decaying into neutrinos, have also been discussed. It is found that only in a certain jet energy region and with a certain number of extra dimensions can the quantum gravity signal be distinguished from the background, which inversely lead to the effective scale M_D to be probed up to (8.8 ± 0.9) TeV for two extra dimensions and (5.9 ± 0.5) TeV for four extra dimensions with sufficient integrated luminosity, e.g. 100 fb^{-1} , at CERN LHC.

DOI: 10.1103/PhysRevD.78.094002

PACS numbers: 04.50.-h, 04.60.-m, 04.60.Bc, 12.38.Aw

I. INTRODUCTION

It has been purposed that standard model (SM) particles live in the usual $3 + 1$ -dimensional space, while gravity can propagate in a higher-dimension space [1,2]. Such a scenario is helpful to reduce the fundamental mass scale from the large Plank scale down to be about the TeV scale and then to solve the so-called hierarchy problem, so it arouses people's interests since its first announcement. Numerous attempts have been carried out to find the signal of the large extra dimension, i.e. measurements of gravity at short distances, studies of various astrophysical and cosmological implications of large extra dimension, and collider searches for virtual and real graviton effects [3–10]. The CERN LHC, with its high collision energy (14 TeV) and high luminosity ($10^{34} \text{ cm}^{-2} \text{ s}^{-1}$), shall provide a better platform to study the extra-dimension phenomenology both experimentally and theoretically.

The leading experimental signal of the real graviton at the LHC is from the hadronic process $pp \rightarrow \text{jet} + \cancel{E}_T$, where \cancel{E}_T stands for the transverse missing energy. We shall present a detailed discussion on the hadronic production of the graviton through the hard subprocesses: $q\bar{q} \rightarrow G + g$, $g + q \rightarrow G + q$, and $g + g \rightarrow G + g$. By using the quantum gravity effective theory with large extra dimensions [11,12], we try to study the quantum gravity effects and their dependence on the number of extra dimensions and to study up to what energy scale the LHC can probe.

Furthermore, the main theoretical uncertainty for the graviton production shall be studied, which includes the parton distribution functions (PDFs) for the initial partons, the choice of the factorization scale μ_F^2 , and the typical energy scale Q^2 for the hard scattering amplitude, the number of the extra dimensions for the graviton production, etc.

The processes $q\bar{q} \rightarrow g + Z^0$ and $qg \rightarrow qZ^0$, followed by an invisible decay of Z^0 , i.e. $Z^0 \rightarrow \nu\bar{\nu}$, give an irreducible physical background to graviton production. We refer to these processes as the ‘‘SM background.’’ We will estimate the observability of the graviton signal by comparing its hadronic cross section to that of the SM background. There are other important background sources from mismeasured jets and W production with forward leptons, however, as argued in Ref. [13], these backgrounds decrease sharply as the lower bound on missing E_T is increased, so we shall not consider it here.

The remainder of the paper is organized as follows. Section II is devoted to give the main formulae for graviton production within the framework of the quantum gravity effective theory with large extra dimensions. Numerical results and discussions are presented in Sec. III, where the uncertainties in estimates and a discussion on the value of the effective energy scale M_D shall be presented. The last section is reserved for a summary.

II. CALCULATION TECHNOLOGY

According to the QCD factorization formulae, the hadronic production of the graviton at the collision center-of-mass energy \sqrt{S} can generally be written as

*wuxg@cqu.edu.cn

$$d\sigma(S, E_T, \dots) = \sum_{ij} \iint dx_1 dx_2 F_{H_1, P_1}^i(x_1, \mu_F^2) F_{H_2, P_2}^j(x_2, \mu_F^2) d\hat{\sigma}_{ij \rightarrow \text{jet} + \cancel{E}_T}(P_1, P_2, x_1, x_2, \mu_F^2, Q^2, \hat{s}, \dots), \quad (1)$$

where $F_{H_1, P_1}^i(x_1, \mu_F^2)$ and $F_{H_2, P_2}^j(x_2, \mu_F^2)$ are PDFs of incoming hadrons H_1 (momentum P_1) and H_2 (momentum P_2) for parton i (with the momentum fraction x_1) and parton j (with the momentum fraction x_2), respectively. Q^2 is the ‘‘characteristic energy scale of the subprocess squared’’ and μ_F^2 is the ‘‘energy scale squared’’ where the factorization about the PDFs and the hard subprocess is made. Usually for leading order (LO) calculation to obtain the best results, the two scales μ_F^2 and Q^2 are carried out as the same, thus later on we take $\mu_F^2 = Q^2$ except in one case when estimating the uncertainty from LO and the ambiguity of the choices about μ_F^2 and Q^2 .

$d\hat{\sigma}_{ij \rightarrow \text{jet} + \cancel{E}_T}$ stands for the differential cross section of the relevant hard subprocess, in which $\hat{s} = x_1 x_2 S$ is the center-of-mass energy of the subprocess and \cancel{E}_T stands for the missing transverse energy. Within the framework of the quantum gravity theory with large extra dimensions, the differential cross section for inclusive graviton (G) production, i.e. $ij \rightarrow Gk$ with i, j , and k stands for corresponding partons, can be written as [12]

$$\frac{d^2}{dt dm} \hat{\sigma}_{ij \rightarrow Gk} = S_{\delta-1} \frac{\bar{M}_P^2}{M_D^{2+\delta}} m^{\delta-1} \frac{d\hat{\sigma}_m}{dt}, \quad (2)$$

where $d\hat{\sigma}_m/dt$ stands for the differential cross section for producing a single Kaluza-Klein graviton of mass m , $\bar{M}_P = M_P/\sqrt{8\pi} = 2.4 \times 10^{18}$ GeV, $S_{\delta-1}$ is the surface of a unit-radius sphere in δ dimensions, for $\delta = 2n$ and n integer, $S_{\delta-1} = 2\pi^n/(n-1)!$ and for $\delta = 2n+1$, $S_{\delta-1} = 2\pi^n/\prod_{k=0}^{n-1}(k+\frac{1}{2})$. For the present $2 \rightarrow 2$ subprocesses, the Mandelstam variables are defined as $s = (p_i + p_j)^2$, $t = (p_i - p_G)^2$, and $u = (p_i - p_k)^2$. Since the graviton interaction vertex is suppressed by $1/\bar{M}_P$, it can be found that $\hat{\sigma}_m \propto \bar{M}_P^{-2}$, and the factor \bar{M}_P^2 appearing from the phase-space summation exactly cancels the Planck mass dependence in Eq. (2). In other words, the large phase space of the Kaluza-Klein modes, corresponding to the large volume of the compactified space, exactly cancels the dependence on \bar{M}_P and gives an effective interaction suppressed only by inverse powers of M_D . This is the reason why sizable contributions from the graviton may be observed at the LHC, and inversely, one can estimate to what energy scale the LHC can probe. For the differential partonic cross sections $d\hat{\sigma}_m/dt$ that produce a single Kaluza-Klein graviton with mass m , we obtain

$$\frac{d\hat{\sigma}_m}{dt}(q\bar{q} \rightarrow gG) = \frac{\alpha_s(Q^2)}{36s\bar{M}_P^2} F_1(t/s, u/s), \quad (3)$$

$$\frac{d\hat{\sigma}_m}{dt}(qg \rightarrow qG) = \frac{\alpha_s(Q^2)}{96s\bar{M}_P^2} F_2(t/s, u/s), \quad (4)$$

$$\frac{d\hat{\sigma}_m}{dt}(gg \rightarrow gG) = \frac{3\alpha_s(Q^2)}{16s\bar{M}_P^2} F_3(t/s, u/s), \quad (5)$$

where Q^2 stands for the characteristic energy scale of the hard scattering amplitude, q stands for the light quarks u, d , and s respectively, and the functions $F_{1,2,3}$ take the following form:

$$F_1(x, y) = \frac{1}{xy} (4xy + z)(1 - 2xy + z^2), \quad (6)$$

$$F_2(x, y) = \frac{1}{xz} (2x - z^2 - y^2)(z + z^2 + x(4 + z)), \quad (7)$$

$$F_3(x, y) = \frac{1}{xz} [x^2 y^2 + 2xy(z^2 - z + 1) + (1 + z + z^2)^2]. \quad (8)$$

The relation $z = 1 + x + y$ is implicitly adopted and can be deduced from the fact that $s + t + u = m^2$. It can be easily found that $F_{1,3}(x, y) = F_{1,3}(y, x)$ as is the requirement of the invariance under exchange of the Mandelstam variables t and u .

For the background subprocesses $ij \rightarrow Z^0 k$, we obtain

$$\frac{d\hat{\sigma}}{dt}(q\bar{q} \rightarrow gZ^0) = \frac{\pi\alpha(Q^2)\alpha_s(Q^2)(L_q^2 + R_q^2)}{9x_W(1-x_W)s^2 tu} \times (m_{Z^0}^4 + s^2 - 2tu), \quad (9)$$

$$\frac{d\hat{\sigma}}{dt}(qg \rightarrow qZ^0) = \frac{\pi\alpha(Q^2)\alpha_s(Q^2)(L_q^2 + R_q^2)}{18x_W(1-x_W)m_{Z^0}^2 s^3 t} \times [6sm_{Z^0}^4 - 2s(s+t)m_{Z^0}^2 + t^3], \quad (10)$$

where $x_W = \sin^2\theta_W$, $R_q = -2e_q x_W$, and $L_q = 1/2 - 2e_q x_W$ with e_q stands for the electric charge of the q quark.

III. NUMERICAL RESULTS AND DISCUSSIONS

In the following, we shall first discuss the uncertainties in estimating the graviton/ Z^0 production. For the LO estimation, we shall concentrate our attention on the main uncertainties, which include the PDFs for the light quarks, the choice of the factorization scale μ_F , and the typical energy scale Q^2 for the hard scattering amplitude and the number of the extra dimensions for the graviton production.

The number of extra dimensions (δ) can either be too small or too large. We are interested in the case in which δ is not too large (say $\delta \lesssim 6$), under such a condition the mass splitting Δm is so small that the sum over the different Kaluza-Klein states can be replaced by a continuous

integration, and then the enormous number of accessible Kaluza-Klein modes can rightly compensate the $1/\bar{M}_P^2$ factor in the scattering amplitude. While an even larger number of extra dimensions shall lead to the mass splitting Δm and become comparable with the experimental energy resolution, hence only a smaller number of Kaluza-Klein modes can be produced, and then the total cross section is negligible due to the unavoidable $1/\bar{M}_P^2$ suppression. On the other hand, it is argued that δ cannot be too small as is required by the latest torsion-balance experiment [14]. Constraints from cosmology also lead to nontrivial bounds on extra dimensions [15,16].¹ So, we take $\delta \in [2, 6]$ to study its effect on the hadronic production.

As is shown in Eq. (1), PDFs $F_{H_1, P_1}^i(x_1, \mu_F^2)$ and $F_{H_2, P_2}^j(x_2, \mu_F^2)$ generate certain uncertainties in the estimation. PDFs are of nonperturbative nature, and in Eq. (1) they have been factorized out at the energy scale μ_F^2 with the help of pQCD factorization theorem. The PDFs can be obtained only through global fitting of the experimental data and evolve them to the requested characteristic scale in a standard way of pQCD, so there are several groups, e.g. CTEQ [19], GRV [20], and MRS [21], etc., who devote themselves to offering accurate PDFs to the world and to keeping PDFs updated with the newly available relevant experimental data. Thus in literature, different versions of PDFs (including different issues by the same group) are used in the estimates of the hadronic production. To be self-consistent with the LO pQCD calculation, we shall adopt the two LO PDFs: CTEQ6L [19] and MRST2001L [21] as typical examples for PDFs. The versions of the gluon distributions ending with “L” are accurate up to the leading logarithm order (LLO), i.e., their QCD evolution effects with α_s running are included, so for the production to show the uncertainties correctly up to LO accuracy, it is necessary for the PDFs, the hard subprocess, and the QCD “coupling constant” α_s “run” to the energy scale Q^2 properly. When computing the production and taking the PDFs from one version of the three groups, the running α_s should also be taken from the same group.

As for the leading order estimation, how to choose the energy scale Q^2 is a very tricky problem. If Q^2 is chosen properly, the results may be quite accurate. From experience, for a hard subprocess with a two-body final state, generally the choice of $Q^2 = \hat{s}/4$ can lead to an accurate LO result. To see the uncertainty caused by different choices of Q^2 , we take two typical types for Q^2 , i.e. Type A: $Q^2 = \hat{s}/4$ with \hat{s} the squared center-of-mass energy of the subprocess; Type B: $Q^2 = M_i^2 \equiv p_i^2 + m^2$, the squared transverse mass of the graviton/ Z^0 , respectively. And furthermore, to see the uncertainties from Q^2 choice, instead of variation on the choices with $Q^2 = \mu_F^2$, the

¹By using the hyperbolic curved other than the flat extra dimensions [17], it has been argued that those cosmology constraints can be naturally satisfied [18].

authors in literature, such as Ref. [22], also try $Q^2 \neq \mu_F^2$ and see the uncertainty. Here following them, we also calculate the distributions with $Q^2 \neq \mu_F^2$. More explicitly, as suggested in Refs. [22,23], we take $\mu_F^2 \in [M_i^2/4, 4M_i^2]$ and $Q^2 \in [M_i^2/4, 4M_i^2]$ simultaneously to do the discussion.

Other parameters like m_{Z^0} , x_W , and the fraction of Z^0 decaying to invisible particles affect the production slightly, so we directly take them to be their center values as adopted in the literature, e.g. $m_{Z^0} = 91.187$ GeV, x_W to be 0.2311, and the fraction of Z^0 decaying to invisible particles like (anti)neutrinos $\nu(\bar{\nu})$ to be the center value of $(20.00 \pm 0.06)\%$ [24].

Another important thing we need to be careful of is the regulation of the cross section to avoid the nonperturbative regime, i.e. to deal with the signatures arising from collisions with parton center-of-mass energies of order M_D or above properly. At $\sqrt{\hat{s}} \gg M_D$, parton collisions are expected to produce classical black holes [25]. As has been pointed out, the discrepancy between the two cases with or without the cut $\hat{s} \leq M_D^2$ shall be increased with the increment of $E_{T,\text{jet}}^{\text{min}}$ and decreased with the increment of M_D [12], therefore by taking proper $E_{T,\text{jet}}$ cut in experimental analysis, one can select different ranges of M_D to probe perturbatively. And numerically, we can find that under the present conditions, with or without the cut $\hat{s} \leq M_D^2$ shall affect our final conclusions slightly, so we shall adopt the cut $\hat{s} \leq M_D^2$ in all the following discussions.

A. The uncertainties in estimates

First, we show the uncertainty caused by the different choice of extra dimensions δ . For the purpose, we fix PDF

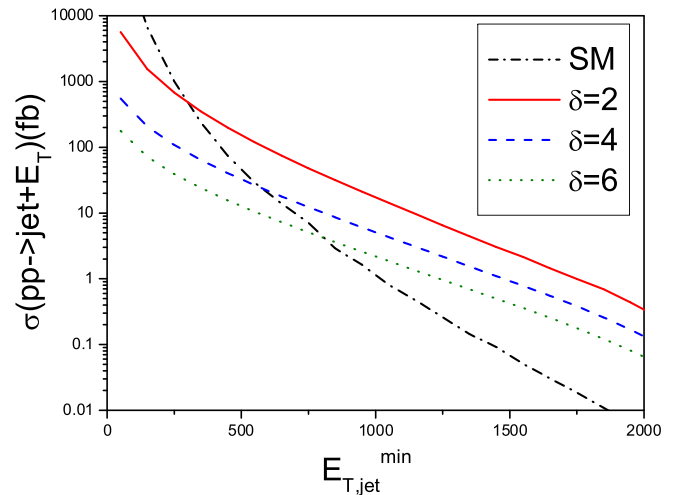


FIG. 1 (color online). Total jet + nothing cross section at the LHC integrated for the requirement that $E_{T,\text{jet}} > E_{T,\text{jet}}^{\text{min}}$ with an acceptance cut on the jet rapidity $|\eta| \leq 3$. The dash-dotted line is the SM background, the solid, dashed, and dotted lines are for $\delta = 2, 4$, and 6, respectively.

to be CTEQ6L, $M_D = 5$ TeV, $Q^2 = \hat{s}/4$, and $\mu_F^2 = Q^2$. We show the signal and the background rates for the transverse jet energy larger than $E_{T,\text{jet}}^{\text{min}}$ in Fig. 1, with an acceptance cut on the jet rapidity $|\eta| \leq 3$. It is shown that the signal rates decrease with the increment of δ . The SM background is bigger than the graviton signal in the lower transverse jet energy region but it drops down much quicker than the signal, and one may distinguish the signal from the background in the large transverse jet energy region. In other words, the large transverse jet energy region shall provide an effective platform to distinguish the signal and the background.

Second, we show the uncertainty from different choices of Q^2 and μ_F^2 . For such a purpose, we fix PDF to be CTEQ6L, $M_D = 5$ TeV, $\delta = 4$. It is found that by taking two choices of Q^2 (type A and type B) under the case of $\mu_F^2 = Q^2$, the uncertainties for both the background and the signal are small, i.e. the differences between these two types of Q^2 are less than 10% for both the background and the signal. Furthermore, we show the case of $\mu_F^2 \neq Q^2$ by shaded band in Fig. 2, with an acceptance cut on the jet rapidity $|\eta| \leq 3$, where $\mu_F^2 \in [M_i^2/4, 4M_i^2]$ and $Q^2 \in [M_i^2/4, 4M_i^2]$. It is found that the largest value is obtained when $\mu_F^2 = M_i^2/4$ and $Q^2 = M_i^2/4$, and the lowest value is obtained when $\mu_F^2 = 4M_i^2$ and $Q^2 = 4M_i^2$. From Fig. 2 one may also observe that while the uncertainty for the background changes to be around 20% (as shown by the thinner shaded band), the uncertainty for the signal can be changed up to 50% (as shown by the thicker shaded band).

Third, we show the uncertainty from different choices of PDFs by fixing $M_D = 5$ TeV, $\delta = 4$, and $\mu_F^2 = Q^2 = \hat{s}/4$. We show the results for two LO PDFs in Fig. 3 with

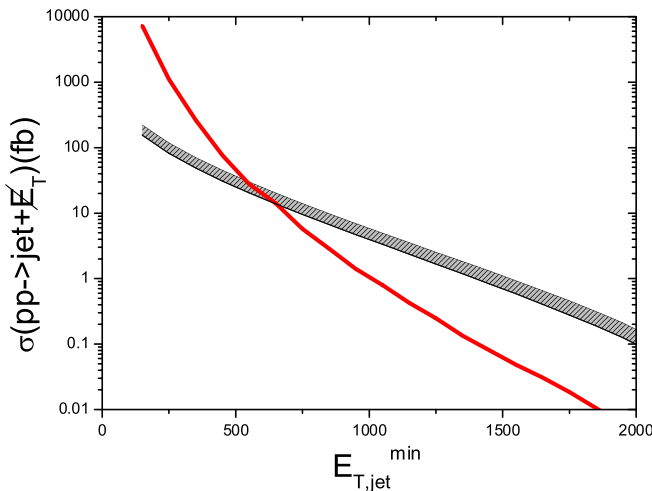


FIG. 2 (color online). Total jet + nothing cross section at the LHC integrated for the requirement that $E_{T,\text{jet}} > E_{T,\text{jet}}^{\text{min}}$ with an acceptance cut on the jet rapidity $|\eta| \leq 3$. The thinner and thicker shaded bands stand for the SM background and the signal, respectively, with the upper edge for $\mu_F^2 = M_i^2/4$ and $Q^2 = M_i^2/4$ and the lower edge for $\mu_F^2 = 4M_i^2$ and $Q^2 = 4M_i^2$.

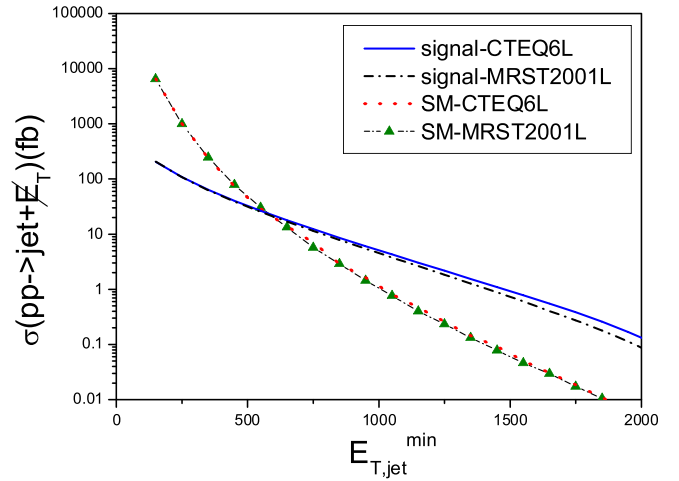


FIG. 3 (color online). Total jet + nothing cross section at the LHC integrated for the requirement that $E_{T,\text{jet}} > E_{T,\text{jet}}^{\text{min}}$ with an acceptance cut on the jet rapidity $|\eta| \leq 3$. Two typical LO PDFs, e.g. CTEQ6L and MRST2001L are adopted.

an acceptance cut on the jet rapidity $|\eta| \leq 3$, i.e. CTEQ6L and MRST2001L. It is found that the results of CTEQ6L and MRST200L are close to each other, i.e. the difference is less than 20%. More explicitly, we show the total jet + nothing cross section $\sigma(pp \rightarrow \text{jet} + \cancel{E}_{T,\text{jet}})$ versus PDFs at the LHC in Table I. Table I shows more explicitly that even though the SM background is bigger than the graviton signal in the lower transverse jet energy region, it drops down quickly, and at $E_{T,\text{jet}}^{\text{min}} \sim 1$ TeV it is less than 25% of the signal. At the present the next-to-leading order (NLO) results are not available,² and to have a rough idea on how the NLO calculation will affect the present results, we take the mismatched NLO PDF as CTEQ6M [19] to do the calculation. It is also found that the results from the mismatched CTEQ6M shall be bigger than that of CTEQ6L by about 25%. So a full NLO estimation shall be helpful to improve our present estimations.

Finally, we show the uncertainty from different choices of M_D by fixing PDF to be CTEQ6L, $\delta = 4$, $Q^2 = \hat{s}/4$, and $\mu_F^2 = Q^2$. We show the signal and the background rates for the transverse jet energy larger than $E_{T,\text{jet}}^{\text{min}}$ in Fig. 4 with an acceptance cut on the jet rapidity $|\eta| \leq 3$. It is shown that the rate decreases with the increment of M_D under the same condition $E_{T,\text{jet}} > E_{T,\text{jet}}^{\text{min}}$.

B. To what energy scale can LHC probe ?

It is found that the SM background changes slightly within the reasonable regions of the above-mentioned uncertain sources, so it can be treated as a basis to decide to what energy scale LHC can probe. Since the large extra dimensions can be probed only when the deviation of the

²Such a NLO calculation is in progress [26].

TABLE I. Total jet + nothing cross section $\sigma(pp \rightarrow \text{jet} + \cancel{E}_{T,\text{jet}})$ (in unit: fb) versus PDFs at the LHC integrated for the requirement that $E_{T,\text{jet}} > E_{T,\text{jet}}^{\min}$ with an acceptance cut on the jet rapidity $|\eta| \leq 3$. Two LO PDFs: CTEQ6L and MRST2001L, and one NLO PDF: CTEQ6M, are adopted.

PDFs	Signal with $E_{T,\text{jet}} > E_{T,\text{jet}}^{\min}$			SM background with $E_{T,\text{jet}} > E_{T,\text{jet}}^{\min}$		
	0.50 TeV	1.0 TeV	1.5 TeV	0.50 TeV	1.0 TeV	1.5 TeV
CTEQ6L	32.	5.1	0.92	46.	1.1	0.070
MRST2001L	31.	4.5	0.73	47.	1.0	0.060
CTEQ6M	40.	6.3	1.1	57.	1.1	0.074

cross section within the framework of the large extra-dimension model from the SM background is large enough, we adopt the 5σ large extra-dimension effect observable limit and 3σ exclusion limit as suggested in the literature [27] to extract the constraint of the fundamental energy scale M_D , i.e.

$$\Delta\sigma = \sigma_{\text{LED}} - \sigma_{\text{Bgd}} \geq \frac{5\sqrt{\sigma_{\text{LED}}\mathcal{L}}}{\mathcal{L}}, \quad (11)$$

$$\Delta\sigma = \sigma_{\text{LED}} - \sigma_{\text{Bgd}} \leq \frac{3\sqrt{\sigma_{\text{LED}}\mathcal{L}}}{\mathcal{L}}. \quad (12)$$

The corresponding M_D sensitivity ranges versus δ are shown in Table II with high integrated luminosity $\mathcal{L} = 100 \text{ fb}^{-1}$, where the cuts $|\eta| \leq 3$ and $E_{T,\text{jet}} > 1.0 \text{ TeV}$ are adopted. It has been found that with integrated luminosity $\mathcal{L} \sim \text{several fb}^{-1}$, the main uncertainty comes from the instrumental background [6–9], which includes both the systematic and the statistical errors. So we have taken a higher integrated luminosity $\mathcal{L} = 100 \text{ fb}^{-1}$ to do our calculation such that the systematic error is dominant. And in doing the calculation, we require that $\sigma_{\text{LED}} > \sigma_{\text{Bkd}}$, since it has been found that the present adopted effective gravity

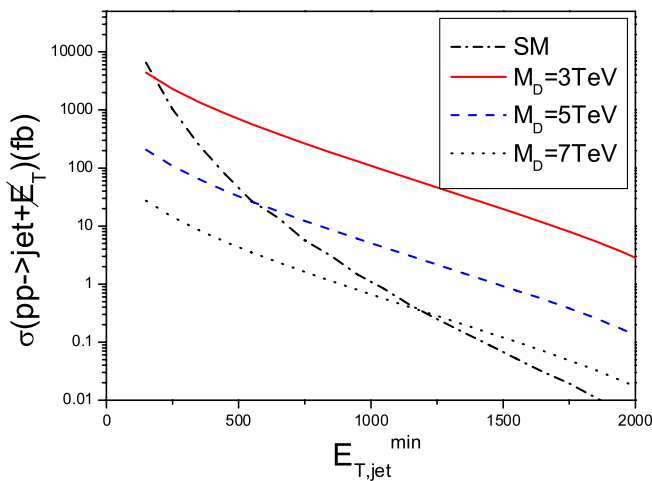


FIG. 4 (color online). Total jet + nothing cross section at the LHC integrated for the requirement that $E_{T,\text{jet}} > E_{T,\text{jet}}^{\min}$ with an acceptance cut on the jet rapidity $|\eta| \leq 3$. Three typical choices for $M_D = 3 \text{ GeV}$, 5 GeV , and 7 GeV are adopted.

theory is mostly reliable in this region as shown in Ref. [12]. It is found that the effective scale M_D can be probed up to $(8.8 \pm 0.9) \text{ TeV}$ for $\delta = 2$, $(5.9 \pm 0.5) \text{ TeV}$ for $\delta = 4$, and $(5.1 \pm 0.3) \text{ TeV}$ for $\delta = 6$, where the center values are obtained by taking CTEQ6L, $Q^2 = \hat{s}/4$ and $\mu_F^2 = Q^2$ and the errors are caused by the above-mentioned main uncertainty sources that varies within their reasonable regions accordingly.

Furthermore, one may observe that the center values for M_D decrease with the increment of δ . Our present results for M_D versus δ with 5σ observable limit as shown in Table II are consistent with the values of maximum M_D determined in Ref. [12] (Table III is there for the same integrated luminosity $\mathcal{L} = 100 \text{ fb}^{-1}$) within reasonable uncertainties, with the center value of our present one slightly bigger than that of Ref. [12], which is mainly caused by the fact that different criterion was adopted in Ref. [12], i.e. a fixed systematic error that is about 10% is adopted to do the discussion.

It has been argued that [12] if the discrepancy for the results with or without the cut $\hat{s} \leq M_D^2$ becomes larger, then the ultraviolet contributions become important, and then our present estimation may be not under control. Numerically, we find that such discrepancy is small for $\delta \leq 4$ (e.g. it is less than 1% for $\delta = 2$ and 10% for $\delta = 4$) by taking the M_D values listed in Table II, while for even larger δ such discrepancy becomes quite large, e.g. for $\delta = 6$ such a discrepancy is up to 100% by taking $M_D = 5.1 \text{ TeV}$. This shows that our present adopted effective theory may not be fully applicable for such a large extra dimension. One may hope to decrease such a discrepancy by lowering the value of $E_{T,\text{jet}}^{\min}$ since a smaller $E_{T,\text{jet}}^{\min}$ leads to

TABLE II. Corresponding M_D sensitivity ranges versus δ with the high integrated luminosity $\mathcal{L} = 100 \text{ fb}^{-1}$. $M_D(3\sigma)$ stands for the 3σ exclusion limit and $M_D(5\sigma)$ stands for the 5σ observable limit, where the center values are obtained by taking CTEQ6L, $Q^2 = \hat{s}/4$, and $\mu_F^2 = Q^2$ and the errors are caused by the above-mentioned main uncertainty sources.

δ	$M_D(3\sigma\text{-exclusion})$	$M_D(5\sigma\text{-observable})$
2	$9.2 \pm 0.7 \text{ TeV}$	$8.8 \pm 0.9 \text{ TeV}$
4	$6.1 \pm 0.5 \text{ TeV}$	$5.9 \pm 0.5 \text{ TeV}$
6	$5.3 \pm 0.3 \text{ TeV}$	$5.1 \pm 0.3 \text{ TeV}$

TABLE III. Maximum M_D sensitivity versus δ with the low integrated luminosity $\mathcal{L} = 10 \text{ fb}^{-1}$. The center values are obtained by taking CTEQ6L, $Q^2 = \hat{s}/4$, and $\mu_F^2 = Q^2$ and the errors are caused by the above-mentioned main uncertainty sources.

δ	2	4	6
Max M_D	$8.2 \pm 0.5 \text{ TeV}$	$5.7 \pm 0.3 \text{ TeV}$	$4.9 \pm 0.2 \text{ TeV}$

a smaller discrepancy, however by doing this, the probed M_D sensitivity range shall only be slightly lowered due to the fact that $E_{T,\text{jet}}^{\text{min}}$ cannot be set too small otherwise it will be more difficult to distinguish the signal from the background, as has been shown in the last subsections that the background shall increase much more quickly than the signal with a decreasing $E_{T,\text{jet}}^{\text{min}}$.

It may be also interesting to make a discussion on the maximum M_D sensitivity with smaller integrated luminosity, e.g. 10 fb^{-1} . Under such a case both symmetric and statistical errors are comparable, and now the criterion (11) and (12) are not applicable, so we adopt the criterion suggested by Ref. [12] to do the discussion, i.e. we add the two errors in quadrature and require

$$\sigma_{\text{LED}} > \sqrt{2} \frac{5\sqrt{\sigma_{\text{Bgd}} \mathcal{L}}}{\mathcal{L}}. \quad (13)$$

The corresponding M_D sensitivity ranges versus δ are shown in Table III with lower integrated luminosity $\mathcal{L} =$

10 fb^{-1} , where the cuts $|\eta| \leq 3$ and $E_{T,\text{jet}} > 1.0 \text{ TeV}$ are adopted and the errors are caused by the above-mentioned main uncertainty sources that varies within their reasonable regions accordingly.

IV. SUMMARY

It is found that with sufficient luminosity at the LHC the fundamental gravity scale can be probed up to several TeV, with the precise value depending on the number of extra dimensions. In the present paper, we have presented a detailed discussion on the leading experimental signal of real graviton at the LHC based on the process $pp \rightarrow \text{jet} + \cancel{E}_T$ with the help of the quantum gravity theory with large extra dimensions. The main standard model background to these processes together with their uncertainties have also been discussed. It is found that in the higher transverse jet energy region, e.g. $E_{T,\text{jet}} > 1.0 \text{ TeV}$, and with a certain number of extra dimensions, the quantum gravity signal can be distinguished from the background.

ACKNOWLEDGMENTS

We would like to thank Professor F. Y. Li for helpful discussions. This work was supported in part by the Natural Science Foundation Project of CQ CSTC under Grant No. 2008BB0298 and Natural Science Foundation of China under Grant No. 10805082, and by the grant from the Chinese Academy of Engineering Physics under Grant No. 2008T0401 and Grant No. 2008T0402.

-
- [1] N. Arkani-Hamed, S. Dimopoulos, and G. Dvali, *Phys. Lett. B* **429**, 263 (1998).
 - [2] I. Antoniadis, N. Arkani-Hamed, S. Dimopoulos, and G. R. Dvali, *Phys. Lett. B* **436**, 257 (1998).
 - [3] G. Landsberg (CDF Collaboration and D0 Collaboration), arXiv:hep-ex/0412028.
 - [4] T. G. Rizzo, *Phys. Rev. D* **59**, 115010 (1999).
 - [5] Y. Uehara, *Mod. Phys. Lett. A* **17**, 1551 (2002).
 - [6] T. Aaltonen *et al.* (CDF Collaboration), arXiv:0807.3132 [*Phys. Rev. Lett.* (to be published)].
 - [7] V. M. Abazov *et al.* (Do Collaboration), *Phys. Rev. Lett.* **101**, 011601 (2008).
 - [8] S. S. Yu (CDF Collaboration and D0 collaboration), arXiv:0807.3523.
 - [9] S. Shmatov (CMS Collaboration), *Nucl. Phys. B, Proc. Suppl.* **177**, 330 (2008).
 - [10] M. Perelstein, arXiv:0809.1843.
 - [11] T. Han, J. D. Lykken, and R. J. Zhang, *Phys. Rev. D* **59**, 105006 (1999).
 - [12] G. F. Giudice, R. Rattazzi, and J. D. Wells, *Nucl. Phys. B* **544**, 3 (1999).
 - [13] E. A. Mirabelli, M. Perelstein, and M. E. Peskin, *Phys. Rev. Lett.* **82**, 2236 (1999).
 - [14] D. J. Kapner *et al.*, *Phys. Rev. Lett.* **98**, 021101 (2007).
 - [15] L. J. Hall and D. Smith, *Phys. Rev. D* **60**, 085008 (1999); V. D. Barger, T. Han, C. Kao, and R. J. Zhang, *Phys. Lett. B* **461**, 34 (1999).
 - [16] Steen Hannestad and Georg G. Raffelt, *Phys. Rev. D* **67**, 125008 (2003); **69**, 029901(E) (2004).
 - [17] N. Kaloper, J. March-Russell, G. D. Starkman, and M. Trodden, *Phys. Rev. Lett.* **85**, 928 (2000).
 - [18] G. D. Starkman, D. Stojkovic, and M. Trodden, *Phys. Rev. Lett.* **87**, 231303 (2001); H. Melbeus and T. Ohlsson, *J. High Energy Phys.* **08** (2008) 077.
 - [19] J. Pumplin, D. R. Stump, J. Huston, H. L. Lai, P. Nadolsky, and W. K. Tung, *J. High Energy Phys.* **07** (2002) 012.
 - [20] M. Glueck, E. Reya, and A. Vogt, *Eur. Phys. J. C* **5**, 461 (1998).
 - [21] A. D. Martin, R. G. Roberts, W. J. Stirling, and R. S. Thorne, *Eur. Phys. J. C* **23**, 73 (2002).
 - [22] M. Klasen, B. A. Kniehl, L. N. Mihaila, and M. Steinhauser, *Phys. Rev. Lett.* **89**, 032001 (2002).

- [23] C. H. Chang, J. X. Wang, and X. G. Wu, *Phys. Rev. D* **70**, 114019 (2004).
- [24] C. Amsler *et al.* (Particle Data Group), *Phys. Lett. B* **667**, 1 (2008).
- [25] D. Bourilkov (ATLAS Collaboration and CMS Collaboration), arXiv:0807.4960; M. Cavaglia, R. Godang, L. M. Cremaldi, and D. J. Summers, *J. High Energy Phys.* 06 (2007) 055.
- [26] X. G. Wu *et al.*, The next-to-leading order estimation of the monojet graviton signal at LHC (unpublished).
- [27] H. Sun, R. Y. Zhang, P. J. Zhou, W. G. Ma, Y. Jiang, and L. Han, *Phys. Rev. D* **71**, 075005 (2005).